Full-band modeling of AM and FM interband cascade laser frequency combs

M. Povolotskyi,[1] I. Vurgaftman[2]
[1] *Jacobs, Hanover, MD 21076, USA*
[2] *Code 5613, Naval Research Laboratory, Washington, DC 20375, USA*

Compact and efficient mid-infrared (MIR) frequency combs are expected to find widespread use in chemical sensing applications, such as on-chip spectroscopy of toxic substances [1]. While most of the experimental MIR laser comb work has involved quantum cascade lasers (QCLs), interband cascade lasers (ICLs) operate cw at room temperature in the 3-4 μm spectral range, which remains difficult for QCLs, and also promise significant reductions in the operating power throughout the MIR spectral range. Furthermore, owing to the long carrier lifetime in an ICL, both passive mode-locking with short pulses (AM) and quasi-cw (FM) comb generation should be possible.

In spite of these promising characteristics, only FM combs based on ICLs have been demonstrated to date. In order to clarify the physical requirements for both AM and FM operation, we have developed a multiscale numerical model that efficiently solves the Maxwell-Bloch equations for the full subband dispersion in the ICL's active type-II wells over a time period of μs. We compare the results of this model to those derived from the two-level approximation relevant to QCLs [2], and evaluate the importance of such parameters as the second-order and higher-order group velocity dispersions, saturable absorber length and recovery time, ambipolar diffusion coefficient, and polarization relaxation time (homogeneous gain broadening linewidth). We determine the optimal design parameters for experimentally demonstrating both passively mode-locked and FM ICL combs, and outline how they can be realized in practice.

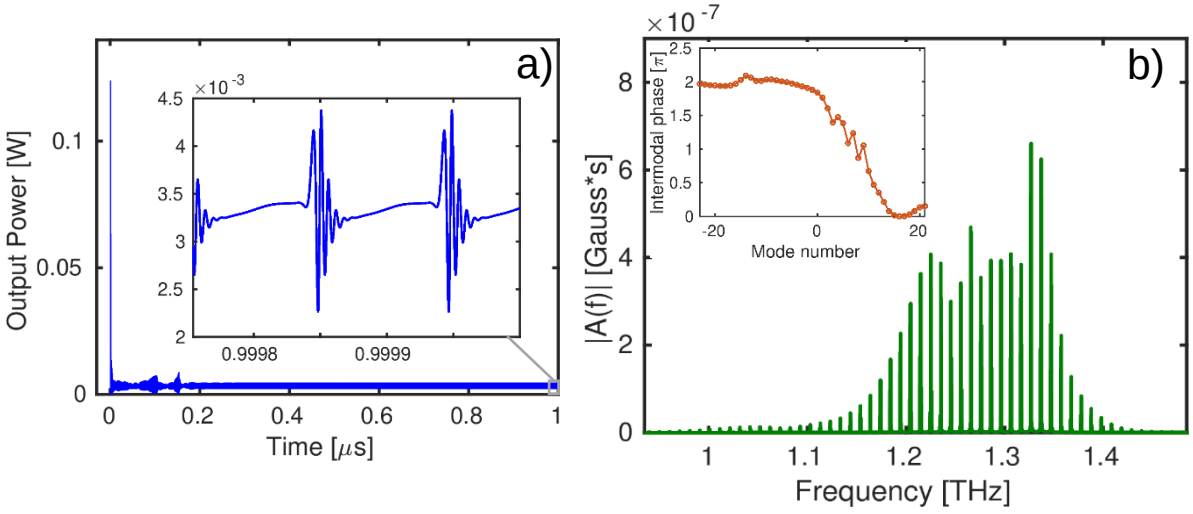

Figure 1. Frequency comb output due to the frequency modulation in an ICL: a) output power; b) output signal modulation spectrum and the intermodal phase difference.

[1] Sterczewski, L. A. *et al*, Opt. Lett. 44, 2113 (2019). [2] Opačak, N. *et al*, Phys. Rev. Lett. 123, 243902(2019).
[+] Author for correspondence: I. Vurgaftman, e-mail: MWIR_laser@nrl.navy.mil

Supplementary Pages

The electromagnetic field is simulated in the slowly varying envelope function approximation, which allows us to use a coarse mesh with points separated by $h > \frac{\lambda}{n_r} \approx 1\ \mu$m, and corresponding time steps $\tau = h/v_g$:

$$\pm\partial_z A^{\pm} + \left(\frac{1}{v_g}\partial_t A^{\pm}\right) + i\frac{\beta_2}{2}\partial_{t^2}^2 A^{\pm} + i^2\frac{\beta_3}{6}\partial_{t^3}^3 A^{\pm} + \ldots + i^{n-1}\frac{\beta_n}{n!}\partial_{t^n}^n A^{\pm} = i\frac{4\pi\omega^2}{\left(\frac{2\pi n_r}{\lambda}\right)c^2}\left(\frac{\Gamma}{w}\right)\left(\frac{2}{(2\pi)^2}\right)P^{\pm} - \frac{\alpha}{2}A^{\pm}, \quad (1)$$

where $A^{\pm}$ are the counter-propagating electric-field amplitudes, $\beta_i = \mathrm{Re}(d^i k/d\omega^i)$ are the group-velocity dispersion (GVD) coefficients, Γ is the mode overlap factor, w is the well width, $P^{\pm}$ are the amplitudes for dipole polarization and α is the absorption coefficient.

The ICL active region is based on a type-II quantum-well heterostructure. Contrary to QCLs, the optical transition energy varies significantly with the electron/hole in-plane wavevector k, so the dipole polarization is a sum of contributions of different k: $P^{\pm} = \int_0^{K\max} d^*(k)\,p^{\pm}(k)(2\pi k)dk$, where $d(k)$ and $p(k)$ are the dipole moment and polarization, respectively. Therefore, to model an ICL it is necessary to know the distribution of electrons and holes over the Brillouin zone at any moment in time. Modeling a non-equilibrium electron gas distribution in both real and momentum space is still a challenging task, so four major assumptions have been made: (1) local charge neutrality; (2) electrons and holes are confined in one direction only, with their transport being quasi-1D along the ICL cavity axis (Fig. S1a); (3) rapid intraband thermalization, meaning both electrons and holes obey the local quasi-Fermi-Dirac distribution; and (4) the spatial dependence of the carrier distribution function along the cavity is approximated as the sum of a large slow-varying envelope $n_0(z)$ and a small first harmonic $n_1(z)$ that oscillates with period $0.5\lambda/n_r$[2]:

$$n^c(z) = n^v(z) = n(z);\ n(z) = n_0(z) + \mathrm{Re}\left(n_1(z)e^{-i\frac{4\pi n_r}{\lambda}z}\right);\ \mu(z) = \mu_0(z) + \mu_1(z);\ \mu_1(z) = \frac{\mu_0(n_0)}{\partial n_0}n_1(z);$$

$$n_{0,1}^{c,v}(z) = \int_0^{K\max} f_{0,1}^{c,v}(k,z)\left(2\cdot 2\pi k\right)dk;\ f_0^{c,v}(k,z) = \frac{1}{\exp\left(\frac{E_{c,v}(k) - \mu_0^{c,v}(z)}{kT}\right)+1};\ f_1^{c,v}(k,z) = \frac{\partial f_0(k,z)}{\partial \mu_0}\mu_1(z) \quad (2)$$

where $\mu(z)$ is the position-dependent quasi-Fermi level.

Starting from these assumptions, a set of equations has been developed in which the quasi-Fermi levels are obtained from the particle conservation law, with the inclusion of uniform injection current, stimulated emission, and Auger nonradiative recombination.

$$\frac{\partial n_0}{\partial t} = \frac{2}{(2\pi)^2}\int_0^{K\max} 2\pi k\left(\frac{\partial f_0}{\partial t}\right)_{rad}dk - \gamma n_0^3 - \frac{n_0}{\tau(z)} + J(z) \quad (3)$$

$$\frac{\partial n_1}{\partial t} = \frac{2}{(2\pi)^2}\int_0^{K_{\max}} 2\pi k\left(\frac{\partial f_1}{\partial t}\right)_{rad}dk - 3\gamma n_0^3 n_1 - \frac{n_1}{\tau(z)} - 4D_a\left(\frac{2\pi}{\lambda}\right)^2 n_1, \quad (4)$$

where $J(z)$ is the injection current density, $1/\tau(z)$ is the defect-assisted recombination rate, which is assumed significant only in an ion-bombarded saturable absorber, D_a is the ambipolar diffusion constant, γ is the Auger recombination constant, and $(\partial f/\partial t)_{rad}$ is the momentum-resolved recombination rate for stimulated emission:

$$\left(\frac{\partial f_0(k)}{\partial t}\right)_{rad} = -\mathrm{Im}\left(\frac{d(k)}{\hbar}\left(p^{+*}(k)A^{+} + p^{-*}(k)A^{-}\right)\right); \quad \left(\frac{\partial f_1(k)}{\partial t}\right)_{rad} = \frac{1}{2}\frac{d(k)}{\hbar}\left(i\left(A^{+}p^{-*}(k) - A^{-*}p^{+}(k)\right)\right) \tag{5}$$

The momentum-resolved polarization components obey the Bloch equations:

$$\partial_t p^{\pm}(k,z,t) = i\left(\left(E_c(k) - E_v(k)\right)/\hbar - \omega\right)p^{\pm}(k,z,t)$$
$$-i\left(\frac{d(k)}{\hbar}\left(A^{\pm}(z,t)\left(f_0^c(k,z,t) - f_0^v(k,z,t)\right) + A^{\mp}(z,t)\left(f_1^c(k,z,t) - f_1^v(k,z,t)\right)\right)\right) - \frac{p^{\pm}(k,z,t)}{T_2}, \tag{6}$$

where T_2 is the polarization relaxation time constant.

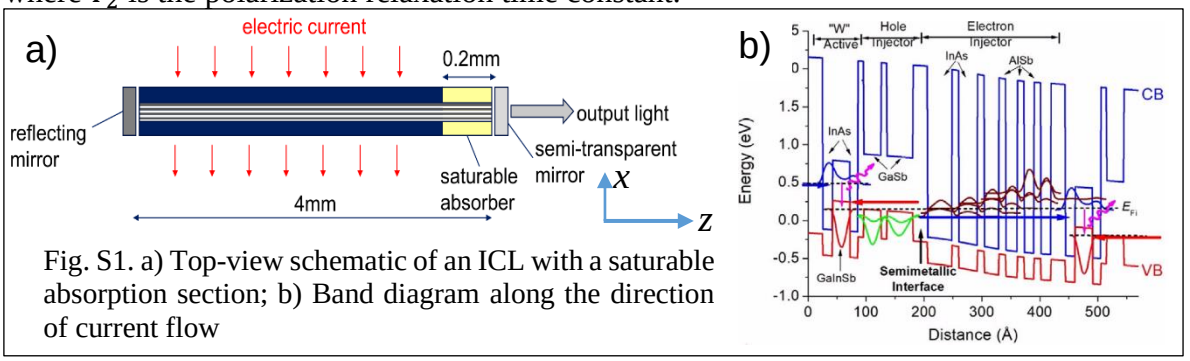

Fig. S1. a) Top-view schematic of an ICL with a saturable absorption section; b) Band diagram along the direction of current flow

The model uses as input the electron and hole subband dispersions in the type-II active InAs/GaInSb/InAs ("W") active region, computed in the 8-band **k·p** approximation (Fig. S1b). In the simulation model, only optical transitions with transition energies close to the photon energy are explicitly considered. It is sufficient to follow the electron and hole distributions in the lowest conduction and highest valence band subbands in the active region, because higher-lying subbands are separated by energies much larger than kT in these thin-layer active regions. The simulation results for an ICL with a saturable absorber are shown in Fig. S2, which shows the formation of an AM frequency comb under optimized conditions.

Numerical simulations suggest that passive mode locking in an ICL comb with a saturable absorber region integrated into the optical cavity can be achieved if the saturated absorption recovers faster than the photon round trip time. While the GVD affects both the spectral and temporal widths of the pulses, the GVD values that are currently achievable experimentally appear sufficient to realize passive mode locking.

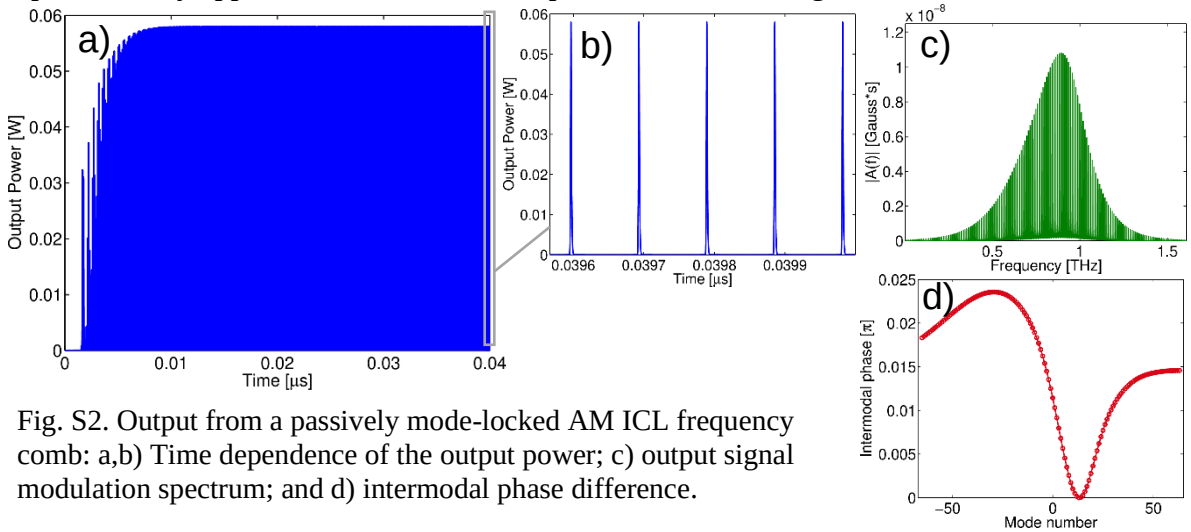

Fig. S2. Output from a passively mode-locked AM ICL frequency comb: a,b) Time dependence of the output power; c) output signal modulation spectrum; and d) intermodal phase difference.